Geophysical Research Letters

RESEARCH LETTER
10.1029/2020GL088339

Key Points:
- In spite of the Antarctic sea ice loss reported in recent years, climate models still fail to capture the observed sea ice trend
- The source of discrepancy resides in the models' forced response, not in their ability to capture the internal variability
- The models' inability to capture the observed sea ice trends is associated with a bias in simulating recent surface heat flux trends

Supporting Information:
- Supporting Information S1

Correspondence to:
R. Chemke,
rc3101@columbia.edu

Citation:
Chemke, R., & Polvani, L. M. (2020). Using multiple large ensembles to elucidate the discrepancy between the 1979–2019 modeled and observed Antarctic sea ice trends. *Geophysical Research Letters*, *47*, e2020GL088339. https://doi.org/10.1029/2020GL088339

Received 10 APR 2020
Accepted 28 JUN 2020
Accepted article online 8 JUL 2020

Using Multiple Large Ensembles to Elucidate the Discrepancy Between the 1979–2019 Modeled and Observed Antarctic Sea Ice Trends

R. Chemke[1] and **L. M. Polvani**[1,2]

[1]Department of Applied Physics and Applied Mathematics, Columbia University, New York, NY, USA, [2]Department of Earth and Environmental Sciences, Lamont-Doherty Earth Observatory, Columbia University, Palisades, NY, USA

Abstract In spite of the unabated emissions of greenhouse gases into the atmosphere, sea ice around Antarctica has increased over most of the satellite era. Such an increase is not captured by climate models, which simulate a melting over the same period. Over the last few years, moreover, the observed sea ice trends have drastically changed, and this might act to cancel the models-observations discrepancy. Here we show that in spite of the very recent Antarctic sea ice trend changes, such discrepancy still exists. Analyzing multiple large ensembles of model simulations, we elucidate the origin of the models-observations discrepancy. We show that internal variability cannot account for the discrepancy, which therefore is likely to stem from biases in the models' forced response to the external forcing. These biases, we show, reside in thermodynamic ocean-atmosphere coupling, as models fail to simulate the trends in surface heat fluxes from reanalyses over the period 1979–2019.

1. Introduction

Projected changes in Antarctic sea ice have large impacts affecting the climate system not only in the Southern Hemisphere (e.g., England et al., 2018) but also deep into the tropics (England et al., 2020). It is thus crucial to ensure that models adequately simulate recent sea ice trends. Unlike Arctic sea ice, which has dramatically declined in recent decades, Antarctic sea ice has surprisingly, at a small but statistically significant rate around most of the continent (with the exception of the Amundsen/Bellingshausen sector, Parkinson, 2019), increased through most of the satellite era, despite the unabated emissions of greenhouse gases into the atmosphere (e.g., Turner et al., 2015). The observed increase in Antarctic sea ice is not reproduced in climate models, which show a strong decrease over the last several decades (Arzel et al., 2006; Roach et al., 2020; Turner et al., 2015; Zunz et al., 2013). In the last few years, however, a remarkable decline in Antarctic sea ice has been documented (Parkinson, 2019): This raises the question as to whether the discrepancy between modeled and observed sea ice trends still exits.

The recent increase in Antarctic sea ice was argued by previous studies to be part of the large internal variability of the climate system, rather the forced response to external forcings. Notably, several studies have documented that the observed sea ice increase is not associated with the forced response to ozone depletion. Over the late twentieth century, the formation of the ozone hole and its associated changes in the winds were found to decrease the Antarctic sea ice by upwelling deep warm water (e.g., Bitz & Polvani, 2012; Landrum et al., 2017; Sigmond & Fyfe, 2010; Solomon et al., 2015). Thus, the recent changes in the Southern Annular Mode, which are mostly associated with ozone depletion (e.g., Polvani et al., 2011), cannot explain the cooling and sea ice growth in the Southern Ocean over the last several decades (Holland et al., 2017; Lefebvre et al., 2004; Liu et al., 2004; Simpkins et al., 2012).

Further evidence for the importance of internal variability in determining the observed sea ice trends was offered in studies who analyzed both observations and model simulations. First, the modeled internal variability was found to capture the recent observed trend, suggesting that the observed trend need not be part of a forced response to external forcings (Polvani & Smith, 2013; Roach et al., 2020; Zunz et al., 2013). Second, using observations prior to the satellite era, two studies showed the presence of a large multidecadal variability in recent decades over the Southern Ocean (Fan et al., 2014; Gagné et al., 2015). Third, a number of studies have argued that Antarctic sea ice trends are strongly influenced by tropical variability (Meehl et al., 2016; Schneider et al., 2015), at least in certain seasons of the year. Finally, it was suggested that the basal

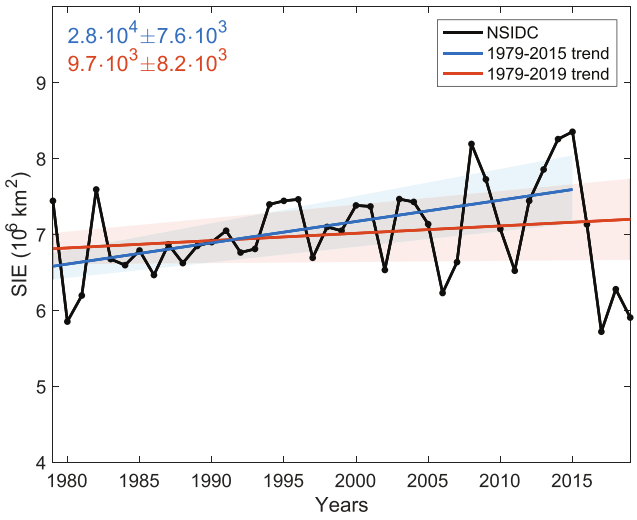

Figure 1. Antarctic MAM SIE time series (10^6 km^2) from NSIDC (black) along with the 1979–2015 (blue) and 1979–2019 (red) linear regressions. Shading shows the standard error of the linear regression, and the slope values are shown in the upper left corner.

melting of the ice shelves might be an important contributor to Antarctic sea ice expansion (Bintanja et al., 2013): That suggestion, however, has not been validated by later, independent, studies (Pauling et al., 2016; Swart & Fyfe, 2013).

The aim of this paper is to shed new light on the discrepancy between modeled and observed sea ice trends. While previous studies have mostly investigated the modeled-observed discrepancy using the Phase 5 of the Coupled Model Intercomparison Program (CMIP5 Taylor et al., 2012), we here investigate it using multiple large ensembles of model simulations. It is imperative to use large ensembles to separate, for each model, the forced response from the internal variability. This approach allows, for the first time, to compare the forced response across several models and therefore to demonstrate where the models' biases reside.

2. Methods

The observed sea ice extent (SIE) from 1979 to 2019 is taken from the National Snow and Ice Data Center (NSIDC, Fetterer et al., 2017), which uses satellite-based multichannel passive-microwave data to estimate monthly means of SIE. For the modeled SIE, we consider 30 CMIP5 models (Taylor et al., 2012) (Table S1 in the supporting information) but only analyze one realization (r1i1p1) for each model, which run between 1850 and 2100 under the historical and RCP8.5 forcings, in order to weigh all models equally.

In addition, to separately quantify the internal variability and the spread in the forced response, we analyze five initial-condition large ensembles of model simulations: the CESM Large Ensemble (CESM-LE) consisting of 40 members (Kay et al., 2015), the CanESM Large Ensemble (CanESM-LE) consisting of 50 members (Kirchmeier-Young et al., 2017), the MPI Grand Ensemble (MPI-GE) consisting of 100 members (Maher et al., 2019), and the CSIRO Large Ensemble (CSIRO-LE) (Jeffrey et al., 2013) and the ESM2M Large Ensemble (ESM2M-LE) (Rodgers et al., 2015) each consisting of 30 members. Output of these CMIP5-class models was obtained from the Multi-Model Large Ensemble Archive, and while all members in each ensemble are subjected to similar historical and RCP8.5 forcings, they are initialized differently: This allows one to estimate the internal variability (as each member exhibits a different transient evolution). Note that while in some of the ensembles the different initial conditions were imposed using a minor perturbation to air temperature, but with an identical ocean state (e.g, CESM), in others, the different initial conditions resulted from selecting different initial years from a preindustrial run, thus starting from different atmosphere and ocean states (e.g., MPI and CSIRO). We also make use of each model's preindustrial control run (forced by the 1850 radiative forcing).

Finally, SIE is computed by summing the area of all model and observed grid cells in the Southern Hemisphere with sea ice concentrations greater than 15% (Fetterer et al., 2017). We focus on the four decades 1979–2019, and all results below are shown for March-April-May (MAM), since these months show the largest Antarctic SIE trends over the last decades (Landrum et al., 2017; Parkinson, 2019; Polvani & Smith, 2013; Turner et al., 2015).

3. The Role of Internal Variability in Recent Sea Ice Trends

We start by recalling, in Figure 1, the behavior of observed Antarctic SIE over the last four decades (black line). From 1979 to 2015 Antarctic SIE increased at a rate of $2.8{\cdot}10^4$ km^2 year^{-1} (blue line). As discussed above, such an increase is surprising, given the monotonic increase in the concentrations of greenhouse gases in the atmosphere. After 2015, however, the SIE has remarkably declined (Parkinson, 2019), thus reducing the linear trend of Antarctic SIE by ~65% (to $9.7{\cdot}10^3$ km^2 year^{-1} from 1979 to 2019, red line). Several studies (e.g., Meehl et al., 2019; Schlosser et al., 2018; Stuecker et al., 2017; Turner et al., 2017; Wang et al., 2019) have argued that oceanic and atmospheric variability may have caused strong decline of sea ice in 2016. However, whether similar mechanisms apply for all years from 2016 to 2019 or whether the post-2015 decline in SIE constitutes the first sign of a forced response to anthropogenic emissions remains

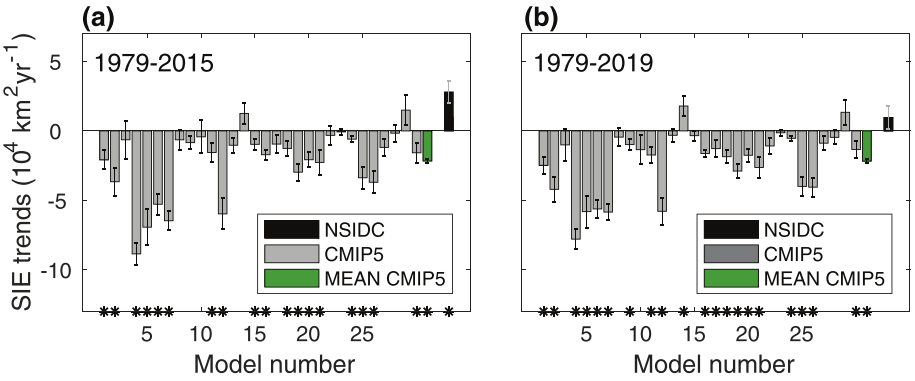

Figure 2. Antarctic MAM SIE (a) 36-year (1979–2015) and (b) 40-year (1979–2019) trends (10^4 km^2 year^{-1}) from NSIDC (black) and CMIP5 models (gray colors, multimodel mean in green). The asterisks indicate that the trends are statistically significant (*p* values lower than 0.05), and the error bars show the standard error of linear regression coefficient.

an open question. Furthermore, since nearly all models simulate melting of SIE over recent decades, the unprecedented decrease in SIE after 2015 suggests that the discrepancy between models and observations may no longer exist.

To quantify the discrepancy between modeled and observed sea ice trends, we separately compute, in Figure 2, their trends from 1979 to 2015 (panel a) and from 1979 to 2019 (panel b). First, the observed increase in SIE between 1979 and 2015 (black bar in panel a) is not simulated by any CMIP5 model: Most models (gray bars, multimodel mean in green) show melting of sea ice (a decline of $-2.16{\cdot}10^4$ km^2 year^{-1} in the multimodel mean). Second, in spite of the strong decline in SIE since 2015, over the entire 1979–2019 period, most models (expect for two, multimodel mean trend of $-2.17{\cdot}10^4$ km^2 year^{-1}) still do not capture the observed, smaller, increase in SIE. It is important to note that even in the new generation of climate models (CMIP6), the discrepancy between modeled and observed sea ice trends remains: Most CMIP6 models show melting of sea ice over recent decades (Roach et al., 2020).

Next, we ask, does the inability of most models to simulate the observed SIE trend stem from biases in the models' internal variability or from biases in their forced response? To answer that, we turn to the five large ensembles described in section 2. Before looking at SIE trends in these ensembles, we examine the ensembles' SIE climatology (the 1979–2019 period), to ensure it is in reasonable agreement with observations. Figure S1 shows the climatological monthly SIE in observations (black) and in all members of each ensemble (each ensemble is plotted with a different color). While the CESM-LE (green lines), CanESM-LE (red lines), and CSIRO-LE (blue lines) models are in reasonable agreement with observations, the MPI-GE (purple lines) and ESM2M-LE (yellow lines) substantially underestimate the Antarctic SIE in all months. Thus, for the remainder of this manuscript we will focus only on the three ensembles (CESM-LE, CanESM-LE, and CSIRO-LE), which are capable of simulating the observed SIE climatology (i.e., within 30% of the observed annual and MAM climatological values).

For these three, the probability density function (PDF) of the 1979–2019 MAM SIE trends is shown in Figures 3a–3c (gray bars), along with each ensemble's mean (green lines), and with the observed trend (brown lines). First, note that, as for the multimodel mean of the CMIP5 in Figure 2b, the mean of each LE also exhibits a negative trend in SIE over the last 40 years: $-3.96{\cdot}10^4$ km^2 year^{-1} in CESM-LE (panel a), $-3.29{\cdot}10^4$ km^2 year^{-1} in CanESM-LE (panel b) and $-2.39{\cdot}10^4$ km^2 year^{-1} in CSIRO-LE (panel c). Since the mean of each ensemble averages out the internal variability, this simulated loss of SIE represents each model's forced response over this period. Second, the observed trend falls outside the PDF of each ensemble (compare gray bars and brown lines), suggesting that internal variability is not the source of the models' inability to capture the observed trend. Thus, the models' inability to capture the observed trend is likely to stem from biases in the models' forced response. Similar conclusions regarding the models' inability to capture the observed trends apply to the annual mean SIE (Figures S2 and S3).

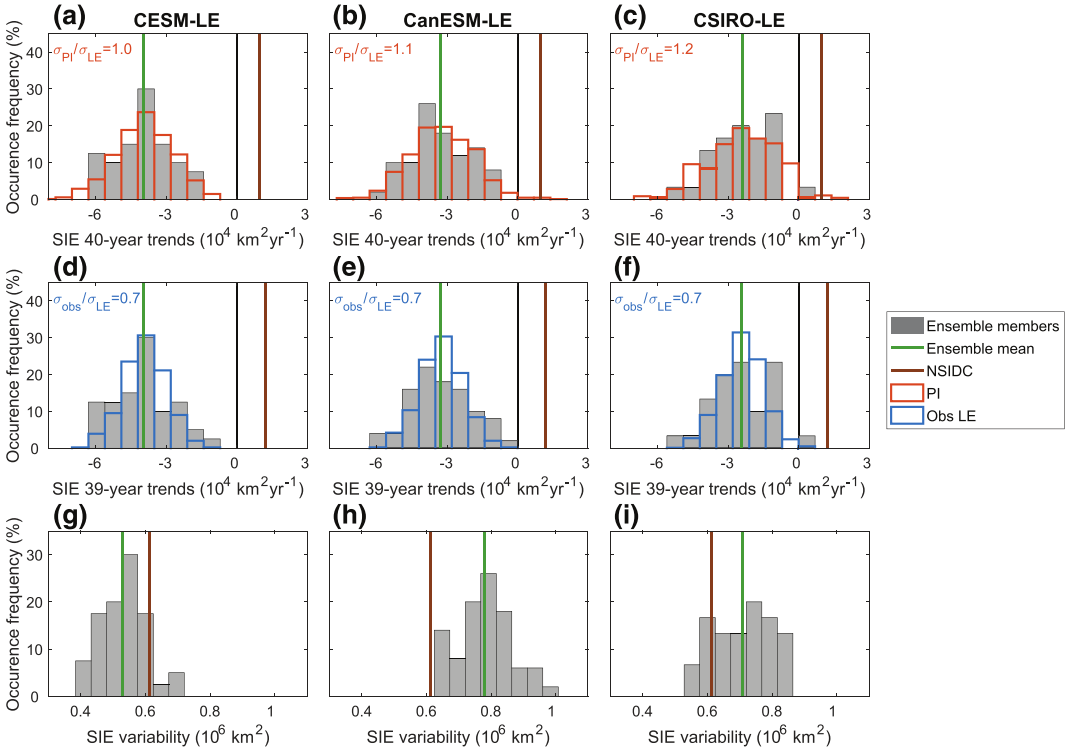

Figure 3. The occurrence frequency (in percentage) of MAM SIE (upper row) 40-year trends (1979–2019), (middle row) 39-year trends (1980–2019), and (bottom row) interannual variability in the large ensembles (gray bars), preindustrial run (red bars), and the observational large ensemble (blue bars). Results for the CESM, CanESM, and CSIRO are shown in the left, middle, and right columns, respectively. The green and brown lines show the mean of each ensemble and the observations (NSIDC), respectively. The ratio between one standard deviation in either the preindustrial (upper row, σ_{PI}) or the observational large ensemble (bottom row, σ_{obs}) and one standard deviation in the large ensemble (σ_{LE}) is shown in each panel's top left corner.

Before concluding that the models are at odds with observations due to biases in the models' forced response, we first need to demonstrate that the models adequately simulate the internal variability of Antarctic SIE. We examine two aspects of the modeled SIE variability in the three ensembles: whether the size of the ensembles is sufficiently large and whether the ensembles adequately simulate the observed variability.

First, we verify whether each ensemble size is sufficiently large by comparing the PDF of 40-year SIE trends from each model to a PDF of SIE trends (of the same lengths) constructed from the respective long preindustrial control run. To do this, we calculate all consecutive (and overlapping) 40-year trends from each models' preindustrial run, which due the length of these runs yields large ensembles: 1,761 members for CESM, 1,056 members for CanESM, and 460 members for CSIRO. Needless to say, the PDF obtained from the preindustrial run is centered on zero (owing to the sole presence of internal variability). We then shift the preindustrial PDF such it is centered on the ensemble mean trend of each model (i.e., on the forced response, green lines in Figures 3a–3c) and examine whether the new PDF (in red) is different than the original one.

The standard deviation of the preindustrial PDF (σ_{PI}) is very close to the standard deviation of the large-ensemble PDF (σ_{LE}): in all three models the ratio σ_{PI}/σ_{LE} is very close to unity (1 for CESM, 1.1 for CanESM, and 1.2 for CSIRO) and is shown in the upper left corners of panels a–c (see Figure S4 for an easy comparison of the two PDFs estimated by fitting a kernel distribution to the data). Thus, adding more members to each ensemble would not have a large impact on the trend's PDF. Moreover, as for the PDF in each of the large ensembles, the preindustrial PDF, centered around the forced trends, also does not capture the observed trend (compare red bars and brown lines): In each control run, less than ~1% of the members capture the observed trend. Thus, we conclude that the size of the large ensembles is sufficiently large to capture the models' SIE variability.

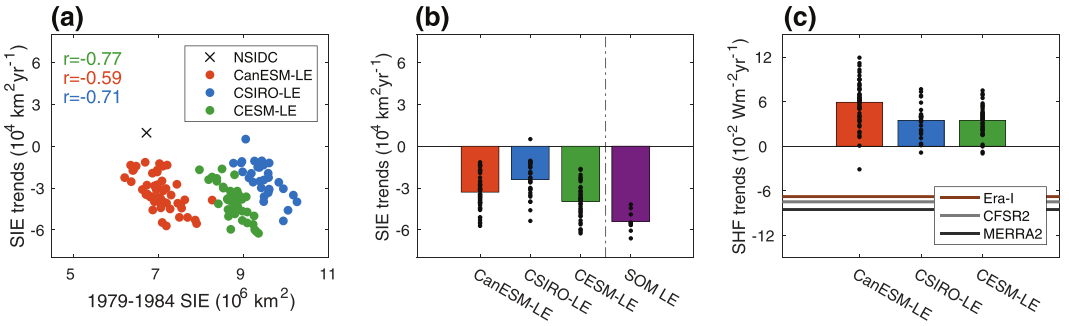

Figure 4. (a) Antarctic MAM SIE 40-year (1979–2019) trends (10^4 km^2 year^{-1}) as a function of the 1979–1984 MAM SIE (10^6 km^2). Correlations for each ensemble are shown in the upper left corner. (b) The forced response of Antarctic MAM SIE 40-year (1979–2019) trends (10^4 km^2 year^{-1}) in each ensemble and in SOM-LE. (c) The 40-year (1979–2019) MAM trends of Southern Ocean total SHF (10^{-2} Wm^{-2} year^{-1}) in each ensemble. The horizontal lines represent the SHF trends from Era-I, CFSR2, and MERRA2. Trends from MERRA2 are from 1980–2018. The black dots show the trends from the different members.

Second, we examine whether the models adequately simulate the observed variability. Following McKinnon et al. (2017), we compare the large-ensemble PDFs of SIE with an observational PDF. This is done by constructing an "observational large-ensemble" of 1,000 members using a block bootstrapping method applied to the observed SIE (blue bars in Figures 3d–3f, a full description of the methodology is given in the supporting information, and in section 5 in McKinnon et al., 2017).

The standard deviation of the PDF of the observational large ensemble (σ_{obs}) is 0.7 smaller than σ_{LE} in all three models (the ratio, σ_{obs}/σ_{LE}, appears in the upper left corner of panels f–d), suggesting that the simulated ensembles might overestimate the internal variability of SIE trends (see Figure S4 where the PDF are smoothed with a standard kernel, allowing for an easier comparison of the relative width of the distributions). To validate the bootstrapping method, we repeat the above analysis for each member of the large ensemble (i.e., we construct a synthetic large ensemble for each member) and compare the resulting averaged standard deviation (σ_{syn}) to σ_{LE} (purple lines in Figure S4). This allows us to examine whether the bootstrapping method can reproduce the PDF of the initial-condition large ensembles. As for the PDF of the observational large ensemble, the ratio σ_{syn}/σ_{LE} is 0.7 for CESM and 0.8 for both CanESM and CSIRO, suggesting that the bootstrapping method is unable to reproduce the SIE variability of the large ensembles. From this, it follows that using the block bootstrapping method we cannot conclude whether the models adequately capture the internal variability of recent SIE trends.

We finally turn to a simpler metric and simply compare the modeled and observed SIE interannual variability: The interannual variability is computed as the standard deviation of the detrended SIE time series, over the period 1979–2019. As seen in the bottom row of Figure 3, we find that the observed interannual variability falls within the PDF of the large ensemble CESM-LE and CSIRO-LE, whereas CanESM somewhat overestimate the interannual variability of SIE.

In summary, the above analysis shows that the ensembles' size is adequate to capture the spread in the simulated SIE trends and, in two of the three large ensembles, the ensembles are able to capture the SIE interannual variability. Thus, the ensembles' inability to capture the observed SIE trend is likely due to biases in the models' forced response: The simulated melting is too strong, as not a single member in each of the three models reproduced the positive observed trend.

4. Biases in the Forced Sea Ice Response

To understand the biases in the forced response, we next examine three processes that might affect the modeled SIE trends. First, while Zunz et al. (2013) argued that the initial sea ice state has a minor effect on the sea ice trends, Singh et al. (2019) have recently suggested that the initial sea ice/ocean state can greatly affect the sea ice trend. We thus next examine whether the excessive melting of sea ice in models in recent decades

might be a result of the modeled sea ice state at the beginning of the observed trend (i.e., during the late 1970s to early 1980s).

We do this by plotting, in Figure 4a, the 1979–2019 SIE trends versus the SIE average over the 1979–1984 period for each of the three large ensembles (colored dots) and for observations (black cross). First, one can see a relatively good (and negative) correlation between the 1979–1984 SIE and the 1979–2019 trends across the members of each ensemble ($r = -0.77$, $r = -0.59$, and $r = -0.71$ in the CESM-LE, CanESM-LE, and CSIRO-LE, respectively). This suggests that members with more sea ice to begin with melt more sea ice over the entire period, and vice versa. Hence, the inability of the CESM-LE and CSIRO-LE to capture the observed 1979–2019 SIE trend might indeed stem from their high SIE at the beginning of this period: None of their members captures the 1979–1984 observed SIE. For CanESM, however, the initial conditions does not explain its inability to capture the observed trend: The 1979–1984 SIE is comparable to the observations. We conclude that biases in the modeled sea ice state prior to the 1979–2019 period might explain some of the discrepancy between climate simulations and observations in some, but not all, models.

Second, having several large ensembles allows us, for the first time, to compare the forced response across different models and evaluate the role of the different models' physical or numerical formulations in the forced melting of SIE: Unlike the different SIE trends across means of each large ensemble, the different SIE trends in one realization across CMIP5 models might stem from both differences in the models' formulations and from internal variability. The forced SIE trends in the three ensembles are plotted in Figure 4b (red, blue and green bars). The forced signal is negative in all ensembles and varies considerably across them: In CESM the forced sea ice loss is 1.6 times greater than in CSIRO over the 1979–2019 period. Thus, while the different models' formulations would probably not resolve the discrepancy between models and observation, correcting for model biases in the forced response could substantially reduce it.

Third, given the importance of ocean heat transport (OHT) in setting the Southern Ocean surface properties (Armour et al., 2016), we next examine the role of changes in OHT in the forced response of Antarctic SIE in recent decades. We have performed an ensemble of 10 simulations using the slab-ocean version of the CESM (denoted SOM-LE), forced under the same historical and RCP8.5 forcings as for the CESM-LE, but without time-evolving OHT: the Q-flux, which represents the slab-ocean OHT convergence (Bitz et al., 2012), and the mixed-layer depth are kept constant at preindustrial monthly and annual values of the CESM, respectively (the SOM-LE is thus initialized from the same preindustrial climatology as for the CESM-LE; Figure S5). Thus, unlike the CESM-LE, which has an active ocean, in the SOM-LE the SIE response to external forcing is not affected by changes in OHT. Comparing the mean (forced response) of CESM-LE and of SOM-LE isolates the role of changes OHT (its direct and indirect effects via the other climate components) in the recent SIE trends in the CESM: The sole difference between the CESM-LE and SOM-LE is changes in OHT.

Green and purple bars in Figure 4b show the SIE trends over 1979–2019 in the mean of the CESM-LE and SOM-LE, respectively. Given that a large portion of oceanic heat uptake occurs in the Southern Ocean, one would expect that fixing the OHT, which includes the ocean heat uptake, should result in a larger warming of the surface and melting of sea ice. Indeed, the melting of sea ice in SOM-LE ($-5.4{\cdot}10^4\,km^2\,year^{-1}$) is larger than in CESM-LE ($-3.96{\cdot}10^4\,km^2\,year^{-1}$): OHT is responsible for reducing the modeled sea ice loss by 26% ($1.44{\cdot}10^4\,km^2\,year^{-1}$). The melting in CESM-LE, therefore, must stem from either thermodynamic ocean-atmosphere-sea ice coupling or from atmospheric processes alone. Note that the effect of OHT to reduce the sea ice loss does not mean that the modeled OHT may not be a contributor to the biased forced response of SIE (e.g., the models' inability to adequately simulate Southern Ocean convection Zhang et al., 2019), since even if its sign is correct its magnitude might be too small, in comparison to observations, to oppose the melting by thermodynamic coupling. Nevertheless, the large contribution of thermodynamic coupling in melting the modeled sea ice clearly indicates that it is a leading process in the modeled versus observed SIE trend discrepancy.

To further demonstrate that oceanic thermodynamic coupling is a contributor to the biased forced response of Antarctic SIE, Figure 4c shows the 1979–2019 MAM trends in total surface heat flux (SHF, i.e., the thermodynamic ocean-atmosphere coupling: longwave and shortwave radiative fluxes and latent and sensible heat fluxes) over the ice-free region in the Southern Ocean (40°–60° S; these latitudes are chosen to isolate ocean-atmosphere coupling) in the three ensembles and from three different reanalyses (horizontal lines): ECMWF Era-Interim (Dee et al., 2011), CFSR2 (Saha et al., 2014), and MERRA2 (Gelaro et al., 2017). As

in Armour et al. (2016), all three models indeed fail to capture the negative trends of total SHF from the reanalyses (positive values indicate warming of the ocean surface, while negative values indicate cooling). Correcting these model biases by reducing the total SHF (i.e., both the local, at the vicinity of sea ice, and the remote, via atmospheric circulation, effects of SHF to warm the surface) would act to cool the Southern Ocean surface in the models, which might reduce their discrepancy with observations. We recognize, of course, that much caution is needed when computing trends from reanalyses (e.g., Liu et al., 2011). The fact that the climatological latitude dependence of total SHF in reanalyses is in agreement across the three reanalyses and in agreement with the models (Figure S6) suggests that reanalyses might be adequate for assessing the models' total SHF trends (this result is also seen in the annual mean; Figure S6).

5. Conclusions

One of the most puzzling features of climate change in the last decades is the increase in Antarctic sea ice. We here show that in spite of the sea ice loss reported in recent years, climate models, which simulate a melting of sea ice, still fail to capture the observed 40-year trend. Using multiple state-of-the-art large ensembles of model simulations, we elucidate whether this discrepancy between climate models and observations stems from biases in the models' forced response or from biases in the models' internal variability. Our analysis suggests that internal variability is not the source of discrepancy, which therefore is likely due to biases in the models' forced response. Note that since we here focus on the discrepancy between climate models and observations, and not on the origin of the observed trends, our results do not contradict the finding of several previous studies, who pointed to internal variability as the reason for the recent increase of observed Antarctic sea ice (Fan et al., 2014; Jones et al., 2016; Polvani & Smith, 2013).

Further analysis of the large ensembles reveals that (a) the initial sea ice state in models may also explain some of the inability of some of the models to capture the observed sea ice trend and (b) the different models' formulation can significantly reduce the forced response, and thus the discrepancy between climate models and observations, and (c) the models' bias in the forced response of SIE to external forcing (melting) stems from ocean-atmosphere thermodynamic coupling. OHT, on the other hand, acts to increase the sea ice and reduce the melting by 26%, on average, in the models we have analyzed. Our analysis of multiple large ensembles, therefore, points to the parameterization of atmosphere-ocean surface fluxes as the component that needs most attention in order to reduce model biases in SIE.

Data Availability Statement

The NSIDC data are available at https://nsidc.org, the Multi-Model Large Ensemble Archive at https://www.cesm.ucar.edu/projects/community-projects/MMLEA/, the CMIP5 data at https://esgf-node.llnl.gov/projects/cmip5/, the Era-Interim at https://www.ecmwf.int, the CFSR2 at https://rda.ucar.edu/, the MERRA2 at https://esgf.nccs.nasa.gov/projects/create-ip/, and the SOM-LE upon request (rc3101@columbia.edu).

Acknowledgments
This research is founded by a grant from the National Science Foundation to Columbia University.

References

Armour, K. C., Marshall, J., Scott, J. R., Donohoe, A., & Newsom, E. R. (2016). Southern Ocean warming delayed by circumpolar upwelling and equatorward transport. *Nature Geoscience*, *9*, 549–554.

Arzel, O., Fichefet, T., & Goosse, H. (2006). Sea ice evolution over the 20th and 21st centuries as simulated by current AOGCMs. *Ocean Modeling*, *12*(3-4), 401–415.

Bintanja, R., van Oldenborgh, G. J., Drijfhout, S. S., Wouters, B., & Katsman, C. A. (2013). Important role for ocean warming and increased ice-shelf melt in Antarctic sea-ice expansion. *Nature Geoscience*, *6*(5), 376–379.

Bitz, C. M., & Polvani, L. M. (2012). Antarctic climate response to stratospheric ozone depletion in a fine resolution ocean climate model. *Geophysical Research Letters*, *39*, L20705. https://doi.org/10.1029/2012GL053393

Bitz, C. M., Shell, K. M., Gent, P. R., Bailey, D. A., Danabasoglu, G., Armour, K. C., et al. (2012). Climate sensitivity of the Community Climate System Model, Version 4. *Journal of Climate*, *25*, 3053–3070.

Dee, D. P., Uppala, S. M., Simmons, A. J., Berrisford, P., Poli, P., Kobayashi, S., et al. (2011). The ERA-Interim reanalysis: Configuration and performance of the data assimilation system. *Quarterly Journal of the Royal Meteorological Society*, *137*, 553–597.

England, M. R., Polvani, L. M., & Sun, L. (2018). Contrasting the Antarctic and Arctic atmospheric responses to projected sea ice loss in the late twenty-first century. *Journal of Climate*, *31*(16), 6353–6370.

England, M. R., Polvani, L. M., & Sun, L. (2020). Tropical climate responses to projected Arctic and Antarctic sea ice loss. *Nature Geoscience*, *13*(4), 275–281.

Fan, T., Deser, C., & Schneider, D. P. (2014). Recent Antarctic sea ice trends in the context of Southern Ocean surface climate variations since 1950. *Geophysical Research Letters*, *41*, 2419–2426. https://doi.org/10.1002/2014GL059239

Fetterer, F., Knowles, K., Meier, W. N., Savoie, M., & Windangel, A. K. (2017). Sea Ice Index, Version 3. Sea ice extent. Boulder, Colorado USA. NSIDC: National Snow and Ice Data Center. Accessed October 27th 2019.

Gagné, M. A., Gillett, N. P., & Fyfe, J. C. (2015). Observed and simulated changes in antarctic sea ice extent over the past 50 years. *Geophysical Research Letters*, *42*, 90–95. https://doi.org/10.1002/2014GL062231

Gelaro, R., McCarty, W., Suárez, M. J., Todling, R., Molod, A., Takacs, L., et al. (2017). The Modern-Era Retrospective Analysis for Research and Applications, Version 2 (MERRA-2). *Journal of Climate*, *30*, 5419–5454.

Holland, M. M., Landrum, L., Kostov, Y., & Marshall, J. (2017). Sensitivity of Antarctic sea ice to the Southern Annular Mode in coupled climate models. *Climate Dynamics*, *49*(5-6), 1813–1831.

Jeffrey, S., Rotstayn, L., Collier, M., Dravitzki, S., Hamalainen, C., Moeseneder, C., et al. (2013). Australia's CMIP5 submission using the CSIRO Mk3. 6 model. *Austalian Meteorites Oceanography J*, *63*, 1–13.

Jones, J. M., Gille, S. T., Goosse, H., Abram, N. J., Canziani, P. O., Charman, D. J., et al. (2016). Assessing recent trends in high-latitude Southern Hemisphere surface climate. *Nature Climate Change*, *6*, 917–926.

Kay, J. E., Deser, C., Phillips, A., Mai, A., Hannay, C., Strand, G., et al. (2015). The Community Earth System Model (CESM) Large Ensemble Project: A community resource for studying climate change in the presence of internal climate variability. *Bulletin of the American Meteorological Society*, *96*, 1333–1349.

Kirchmeier-Young, M. C., Zwiers, F. W., & Gillett, N. P. (2017). Attribution of extreme events in Arctic Sea ice extent. *Journal of Climate*, *30*(2), 553–571.

Landrum, L. L., Holland, M. M., Raphael, M. N., & Polvani, L. M. (2017). Stratospheric ozone depletion: An unlikely driver of the regional trends in Antarctic sea ice in austral fall in the late twentieth century. *Geophysical Research Letters*, *44*, 11,062–11,070. https://doi.org/10.1002/2017GL075618

Lefebvre, W., Goosse, H., Timmermann, R., & Fichefet, T. (2004). Influence of the Southern Annular Mode on the sea ice-ocean system. *Journal of Geophysical Research*, *109*, C09005. https://doi.org/10.1029/2004JC002403

Liu, J., Curry, J. A., & Martinson, D. G. (2004). Interpretation of recent Antarctic sea ice variability. *Geophysical Research Letters*, *31*, L02205. https://doi.org/10.1029/2003GL018732

Liu, J., Xiao, T., & Chen, L. (2011). Intercomparisons of air-sea heat fluxes over the Southern Ocean. *Journal of Climate*, *24*(4), 1198–1211.

Maher, N., Milinski, S., Suarez Gutierrez, L., Botzet, M., Dobrynin, M., Kornblueh, L., et al. (2019). The Max Planck Institute grand ensemble: Enabling the exploration of climate system variability. *Journal of Advances in Modeling Earth Systems*, *11*, 2050–2069. https://doi.org/10.1029/2019MS001639

McKinnon, K. A., Poppick, A., Dunn-Sigouin, E., & Deser, C. (2017). An "observational large ensemble" to compare observed and modeled temperature trend uncertainty due to internal variability. *Journal of Climate*, *30*(19), 7585–7598.

Meehl, G. A., Arblaster, J. M., Bitz, C. M., Chung, C. T. Y., & Teng, H. (2016). Antarctic sea-ice expansion between 2000 and 2014 driven by tropical Pacific decadal climate variability. *Nature Geoscience*, *9*(8), 590–595.

Meehl, G. A., Arblaster, J. M., Chung, C. T. Y., Holland, M. M., DuVivier, A., Thompson, L., et al. (2019). Sustained ocean changes contributed to sudden Antarctic sea ice retreat in late 2016. *Nature Communications*, *10*, 14.

Parkinson, C. L. (2019). A 40-y record reveals gradual Antarctic sea ice increases followed by decreases at rates far exceeding the rates seen in the Arctic. *Proceedings of the National Academy of Sciences of the United States of America*, *116*(29), 14,414–14,423.

Pauling, A. G., Bitz, C. M., Smith, I. J., & Langhorne, P. J. (2016). The response of the Southern Ocean and Antarctic sea ice to freshwater from ice shelves in an Earth system model. *Journal of Climate*, *29*(5), 1655–1672.

Polvani, L. M., & Smith, K. L. (2013). Can natural variability explain observed Antarctic sea ice trends? New modeling evidence from CMIP5. *Geophysical Research Letters*, *40*, 3195–3199. https://doi.org/10.1002/grl.50578

Polvani, L. M., Waugh, D. W., Correa, G. J. P., & Son, S. W. (2011). Stratospheric ozone depletion: The main driver of twentieth-century atmospheric circulation changes in the Southern Hemisphere. *Journal of Climate*, *24*, 795–812.

Roach, L. A., Dörr, J., Holmes, C. R., Massonnet, F., Blockley, E. W., Notz, D., et al. (2020). Antarctic Sea Ice Area in CMIP6. *Geophysical Research Letters*, *47*, e86729. https://doi.org/10.1029/2019GL086729

Rodgers, K. B., Lin, J., & Frölicher, T. L. (2015). Emergence of multiple ocean ecosystem drivers in a large ensemble suite with an Earth system model. *Biogeosciences*, *12*, 3301–3320.

Saha, S., Moorthi, S., Wu, X., Wang, J., Nadiga, S., Tripp, P., et al. (2014). The NCEP Climate Forecast System Version 2. *Journal of Climate*, *27*, 2185–2208.

Schlosser, E., Haumann, F. A., & Raphael, M. N. (2018). Atmospheric influences on the anomalous 2016 Antarctic sea ice decay. *The Cryosphere*, *12*(3), 1103–1119.

Schneider, D. P., Deser, C., & Fan, T. (2015). Comparing the impacts of tropical SST variability and polar stratospheric ozone loss on the Southern Ocean westerly winds. *Journal of Climate*, *28*(23), 9350–9372.

Sigmond, M., & Fyfe, J. C. (2010). Has the ozone hole contributed to increased Antarctic sea ice extent? *Geophysical Research Letters*, *37*, L18502. https://doi.org/10.1029/2010GL044301

Simpkins, G. R., Ciasto, L. M., Thompson, D. W. J., & England, M. H. (2012). Seasonal relationships between large-scale climate variability and Antarctic sea ice concentration. *Journal of Climate*, *25*(16), 5451–5469.

Singh, H. A., Polvani, L. M., & Rasch, P. J. (2019). Antarctic sea ice expansion, driven by internal variability, in the presence of increasing atmospheric CO_2. *Geophysical Research Letters*, *46*, 14,762–14,771. https://doi.org/10.1029/2019GL083758

Solomon, A., Polvani, L. M., Smith, K. L., & Abernathey, R. P. (2015). The impact of ozone depleting substances on the circulation,temperature, and salinity of the Southern Ocean: An attribution study with CESM1(WACCM). *Geophysical Research Letters*, *42*, 5547–5555. https://doi.org/10.1002/2015GL064744

Stuecker, M. F., Bitz, C. M., & Armour, K. C. (2017). Conditions leading to the unprecedented low Antarctic sea ice extent during the 2016 austral spring season. *Geophysical Research Letters*, *44*, 9008–9019. https://doi.org/10.1002/2017GL074691

Swart, N. C., & Fyfe, J. C. (2013). The influence of recent Antarctic ice sheet retreat on simulated sea ice area trends. *Geophysical Research Letters*, *40*, 4328–4332. https://doi.org/10.1002/grl.50820

Taylor, K. E., Stouffer, R. J., & Meehl, G. A. (2012). An overview of CMIP5 and the experiment design. *Bulletin of the American Meteorological Society*, *93*, 485–498.

Turner, J., Hosking, J. S., Bracegirdle, T. J., Marshall, G. J., & Phillips, T. (2015). Recent changes in Antarctic Sea Ice. *Philosophical Transactions of the Royal Society A*, *373*(2045), 2014,0163–2014,0163.

Turner, J., Phillips, T., Marshall, G. J., Hosking, J. S., Pope, J. O., Bracegirdle, T. J., & Deb, P. (2017). Unprecedented springtime retreat of Antarctic sea ice in 2016. *Geophysical Research Letters*, *44*, 6868–6875. https://doi.org/10.1002/2017GL073656

Wang, G., Hendon, H. H., Arblaster, J. M., Lim, E., Abhik, S., & van Rensch, P. (2019). Compounding tropical and stratospheric forcing of the record low Antarctic sea-ice in 2016. *Nature Communications*, *10*, 13.

Zhang, L., Delworth, T. L., Cooke, W., & Yang, X. (2019). Natural variability of Southern Ocean convection as a driver of observed climate trends. *Nature Climate Change*, *9*(1), 59–65. https://doi.org/10.1038/s41558-018-0350-3

Zunz, V., Goosse, H., & Massonnet, F. (2013). How does internal variability influence the ability of CMIP5 models to reproduce the recent trend in Southern Ocean sea ice extent? *The Cryosphere*, *7*(2), 451–468.